

Mutations in KCNK4 that Affect Gating Cause a Recognizable Neurodevelopmental Syndrome

Christiane K. Bauer,^{1,*} Paolo Calligari,² Francesca Clementina Radio,³ Viviana Caputo,⁴ Maria Lisa Dentici,³ Nadia Falah,⁵ Frances High,⁶ Francesca Pantaleoni,³ Sabina Barresi,³ Andrea Ciolfi,³ Simone Pizzi,³ Alessandro Bruselles,⁷ Richard Person,⁸ Sarah Richards,⁸ Megan T. Cho,⁸ Daniela J. Claps Sepulveda,³ Stefano Pro,³ Roberta Battini,⁹ Giuseppe Zampino,¹⁰ Maria Cristina Digilio,³ Gianfranco Bocchinfuso,² Bruno Dallapiccola,³ Lorenzo Stella,² and Marco Tartaglia^{3,*}

Aberrant activation or inhibition of potassium (K⁺) currents across the plasma membrane of cells has been causally linked to altered neurotransmission, cardiac arrhythmias, endocrine dysfunction, and (more rarely) perturbed developmental processes. The K⁺ channel subfamily K member 4 (KCNK4), also known as TRAAK (TWIK-related arachidonic acid-stimulated K⁺ channel), belongs to the mechano-gated ion channels of the TRAAK/TREK subfamily of two-pore-domain (K2P) K⁺ channels. While K2P channels are well known to contribute to the resting membrane potential and cellular excitability, their involvement in pathophysiological processes remains largely uncharacterized. We report that *de novo* missense mutations in *KCNK4* cause a recognizable syndrome with a distinctive facial gestalt, for which we propose the acronym FHEIG (facial dysmorphism, hypertrichosis, epilepsy, intellectual disability/developmental delay, and gingival overgrowth). Patch-clamp analyses documented a significant gain of function of the identified *KCNK4* channel mutants basally and impaired sensitivity to mechanical stimulation and arachidonic acid. Co-expression experiments indicated a dominant behavior of the disease-causing mutations. Molecular dynamics simulations consistently indicated that mutations favor sealing of the lateral intramembrane fenestration that has been proposed to negatively control K⁺ flow by allowing lipid access to the central cavity of the channel. Overall, our findings illustrate the pleiotropic effect of dysregulated *KCNK4* function and provide support to the hypothesis of a gating mechanism based on the lateral fenestrations of K2P channels.

The human genome contains almost 80 genes encoding potassium (K⁺) channels, which constitute the most diversified class of ion channels with regard to structure and gating characteristics (see OMIM database). Such diversity allows K⁺ channels to serve various functions in both excitable and non-excitable cells.^{1–3} K⁺ channels contribute to the maintenance and stabilization of the resting membrane potential, help to repolarize action potentials, mediate hyperpolarization, and determine cellular electrical activity or even cell proliferation. Moreover, K⁺ channels also efficiently mediate modulations of membrane potential and cell function by controlling the K⁺ flux through the cell membrane in response to multiple signals. Since the membrane potential has a key role in the control of a wide array of cellular processes, including cellular excitability, neurotransmitter release, hormone secretion, and electrolyte transport, it is not surprising that aberrant or impaired K⁺ flux due to hyperactivating or inactivating mutations in genes coding for K⁺ channels underlies a heterogeneous spectrum of human disorders affecting neurotransmission and central nervous system function, cardiac electrophysiology, hormone secretion,

and kidney function.^{2,4–6} Remarkably, the aberrant function of some of these channels has recently been documented to affect development and underlie syndromic disorders.^{7–11} Here, we report on the identification of dominantly acting mutations in *KCNK4* (MIM: 605720), which encodes a two-pore-domain (K2P) K⁺ channel,^{12–14} as the cause of a previously unrecognized syndrome having a distinctive facial gestalt, gingival overgrowth, hypertrichosis, intellectual disability, and epilepsy as major features. *KCNK4*, also known as TRAAK (TWIK-related arachidonic acid-stimulated K⁺ channel), is one of three lipid- and mechano-sensitive K2P channels constituting the TRAAK/TREK subfamily. We provide data indicating that the disease-causing mutations are activating basally and cause impaired sensitivity to mechanical stimuli and arachidonic acid. Finally, we offer molecular dynamics data suggesting the structural mechanism by which these mutations exert their gain of function, providing support to the hypothesis of a gating mechanism based on the lateral fenestrations of K2P channels.

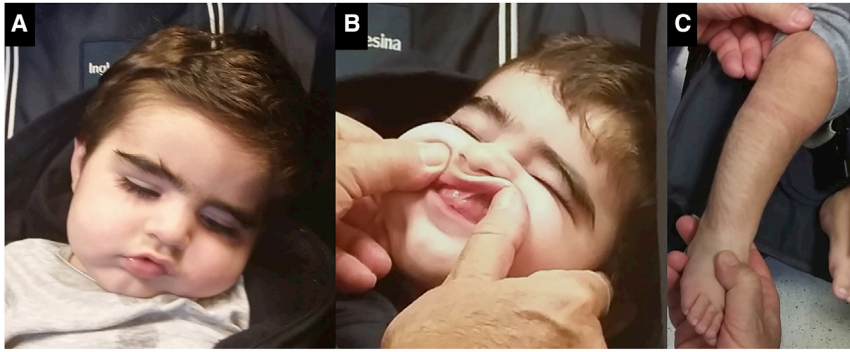
In the frame of a research program dedicated to individuals affected by undiagnosed diseases performed at the

¹Center for Experimental Medicine, Institute of Cellular and Integrative Physiology, University Medical Center Hamburg-Eppendorf, 20246 Hamburg, Germany; ²Department of Chemical Science and Technologies, University of Rome Tor Vergata, 00133 Rome, Italy; ³Genetics and Rare Diseases Research Division, Ospedale Pediatrico Bambino Gesù, IRCCS, 00146 Rome, Italy; ⁴Department of Experimental Medicine, Sapienza University of Rome, 00161 Rome, Italy; ⁵Division of Clinical Genetics, Nemours Children's Hospital, Orlando, FL 32827, USA; ⁶Medical Genetics, Mass General Hospital for Children, Massachusetts General Hospital, Boston, MA 02114-2696, USA; ⁷Department of Oncology and Molecular Medicine, Istituto Superiore di Sanità, 00161 Rome, Italy; ⁸GeneDX, Gaithersburg, MD 20877, USA; ⁹Department of Developmental Neuroscience, IRCCS Stella Maris, 56128 Calambrone, Italy; ¹⁰Center for Rare Disease and Congenital Defects, Fondazione Policlinico Universitario A. Gemelli, IRCCS, Università Cattolica del Sacro Cuore, 00168 Rome, Italy

*Correspondence: cbauer@uke.uni-hamburg.de (C.K.B.), marco.tartaglia@opbg.net (M.T.)
<https://doi.org/10.1016/j.ajhg.2018.09.001>

© 2018 American Society of Human Genetics.

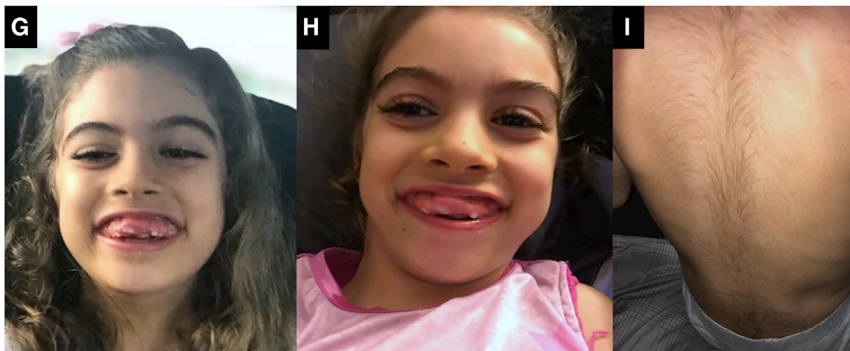




Subject 1 c.515C>A (p.Ala172Glu)



Subject 2 c.730G>C (p.Ala244Pro)



Subject 3 c.515C>A (p.Ala172Glu)

Figure 1. Clinical Features of Individuals with *De Novo* *KCNK4* Mutations

(A–C) Subject 1 (11 months). Note the hypotonic face, bitemporal narrowing, bushy and straight eyebrows, long eyelashes, short deep philtrum, prominent upper and lower vermillion, and receding chin.

(D–F) Subject 2 at 12 months and 5 years. Evolution of facial appearance is appreciable. Note the bitemporal narrowing, bushy and straight eyebrows, long eyelashes, low-set anteverted ears, short deep philtrum, and prominent upper and lower vermillion.

(G–I) Subject 3 at 8 years. Long eyebrows with mild synophris and long eyelashes, thick hair, large mouth with smooth philtrum, and thin lips can be appreciated.

Gingival overgrowth and generalized hypertrichosis occur in all affected individuals with different degree of severity.

a NextSeq500, using paired-end reads. WES data processing, sequence alignment to GRCh37, variant filtering and prioritization by allele frequency, predicted functional impact, and inheritance models were performed using an in-house implemented pipeline, as previously described.^{15–17}

Briefly, reads were aligned to human genome build GRCh37/UCSC hg19 and variants were quality filtered according to GATK's 2016 best practices, annotated, and filtered against public (dbSNP150 and gnomAD v.2.0) and in-house (>1,300 population-matched exomes) databases to retain private and rare (unknown frequency or MAF < 0.1%) variants located in exons with any effect on the coding sequence, and within splice site regions. The functional impact of

Ospedale Pediatrico Bambino Gesù, Rome, the exomes of two unrelated subjects with a molecularly unexplained, clinically superimposable phenotype were scanned to identify the underlying molecular cause. Clinical data and DNA samples were collected from the participating families after written informed consent was obtained, and they were stored and used according to the Institutional Review Board recommendations. In both children, the unusual core of features included variable developmental delay, distinctive facies, gingival overgrowth, hypertrichosis, and EEG anomalies/epilepsy (Figure 1, Table 1, Supplemental Note). Whole-exome sequencing (WES) used DNA samples obtained from leukocytes. Exome capture was attained using the SureSelect Clinical Research Exome v.2 (subject 1) and Nextera v.1.2 (subject 2 and both parents) target enrichment kits, and sequencing was performed on

variants was analyzed by Combined Annotation Dependent Depletion (CADD) v.1.3, M-CAP v.1.0, and InterVar v.0.1.6 algorithms^{18–20} to obtain clinical interpretation according to ACMG 2015 guidelines.²¹ WES data output is reported in Table S1. Two variants in *KCNK4* (subject 1: GenBank: NM_001317090.1; c.515C>A [p.Ala172Glu]; subject 2: GenBank: NM_001317090.1; c.730G>C [p.Ala244Pro]), compatible with autosomal-dominant transmission of the trait, were identified as the only shared events. Both variants were confirmed to occur as *de novo* events by Sanger sequencing. STR analysis confirmed paternity in family 1, and mutation analysis performed on primary skin fibroblasts and hair bulb epithelial cells of both affected subjects supported the germline origin of mutations. One additional subject born to unaffected parents, sharing a similar gestalt, intellectual disability

Table 1. Clinical Features of the Three Subjects with *De Novo* KCNK4 Mutations

	Subject 1	Subject 2	Subject 3
Sex	M	M	F
Age at last evaluation	11 m	5 years 7 m	8 years
KCNK4 mutation (NM_001317090.1)	c.515C>A (p.Ala172Glu)	c.730G>C (p.Ala244Pro)	c.515C>A (p.Ala172Glu)
Inheritance	simplex case, <i>de novo</i>	simplex case, <i>de novo</i>	simplex case, <i>de novo</i>
Pregnancy history	uneventful	uneventful	uneventful
Neonatal feeding/swallowing problems	+	–	+
Growth (at Birth)			
Gestational age	at term	at term	at term
Height	54 cm (75th–90th)	49 cm (25th–50th)	52.07 cm (75th)
Weight	3,925 g (50th–75th)	3,030 g (25th–50th)	3,580 g (50th–75th)
OFC	34 cm (50th–75th)	34 cm (50th–75th)	not available
Growth (at Last Evaluation)			
Height	78 cm (90th–97th)	104 cm (50th)	117.7 cm (10th)
Weight	9.0 kg (25th–50th)	15.5 kg (10th)	21.6 kg (10th)
OFC	43.5 cm (3rd–10th)	51.2 cm (25th)	51.5 cm (10th)
Development Delay			
Global developmental delay	+ ^a	mild speech delay ^b	+ ^c
Intellectual disability	severe	low average	severe
IQ (scale)	not applicable	85 (Griffiths)	not available
Gross motor skills	delayed	not delayed	delayed
Fine motor skills	not applicable	delayed	delayed
Language delay	not applicable	mild	+
Abnormal behavior	not applicable	–	+
Neurological Features			
Seizures/EEG anomalies	EEG anomalies	right focal clonic seizure with secondary generalization	tonic clonic seizure
Hypotonia	+	–	+
Hyperreflexia	+	–	not available
Intention tremor	–	–	+
Visual impairment	nystagmus with bilateral optic hypoplasia	–	nystagmus with bilateral optic hypoplasia
Craniofacial			
Bitemporal narrowing	+	+	–
Blushy eyebrow	+	+	+
Straight eyebrow	+	+	+
Long eyelashes	+	+	+
Low-set ears	+	+	–
Deep philtrum	+	+	–
Short philtrum	+	+	±
Everted upper lip	+	+	+
Thin upper lip	+	+	+
Prominent upper vermilion	+	+	+

(Continued on next page)

Table 1. Continued

	Subject 1	Subject 2	Subject 3
Prominent lower vermilion	+	+	+
Large mouth	–	+	+
Micrognathia/receding chin	+	+	+
Other	–	–	Pierre Robin sequence
Musculo/Skeletal Anomalies			
Brachydactyly	–	–	+
Skin/Ectodermal Features			
Generalized hypertrichosis	+	+	+
Thick hair	+	+	+
Gingival overgrowth	+	+	+
Nail dysplasia	–	–	–

^aThe subject did not reach any milestone at the age of the last evaluation.

^bMajor developmental milestones were achieved within proper age (head control, 3 months; sitting, 7 months; walking, 12 months; single words, 18 months).

^cMajor developmental milestones were delayed (head control, 5 months; crawling, 1 year; walking, around 3 years; single words, 8 years).

(ID), and epilepsy, and carrying the previously identified GenBank: NM_001317090.1 (c.515C>A) as a *de novo* event in the same gene, was found by using the web tool GeneMatcher.²² In this subject, targeted enrichment was attained using the IDT xGen Exome Research Panel v1.0 (affected subject and both parents), and sequencing was performed using a HiSeq4000 platform (Table S1). WES data analysis was performed as previously reported,²³ taking into account the general assertion criteria for variant classification available on the GeneDx ClinVar submission page (submitter code 26957). Variant validation was confirmed by Sanger sequencing. The two variants had not been reported in ExAC/gnomAD, affected residues are conserved among vertebrate orthologs, with Ala²⁴⁴ invariably occurring among members of the TRAAK/TREK subfamily (Figure S1), and were predicted to have a damaging impact on protein function by CADD and M-CAP algorithms (Table S1). In all subjects, WES data analysis excluded the presence of functionally relevant variants compatible with known Mendelian conditions based on the expected inheritance model and clinical presentation (Table S2).

K2P channels are dimeric proteins, with each subunit contributing two pore domains to the channel (Figure 2A).^{13,14,24} Based on available structures of KCNK4, both affected residues mapped in regions possibly involved in KCNK4 activation,^{25–29} with Ala²⁴⁴ located at the center of helix M4 and Ala¹⁷² in M3, in a region of the helix with extensive interaction with M2. Different models of TRAAK/TREK channel gating have been proposed.^{24,27,30–32} According to one hypothesis, channel opening appears to be mediated by a conformational transition of helix M4, causing the closing of two lateral fenestrations exposing the ion-conduction pathway to the hydrophobic core of the lipid membrane.^{27,33} When M4 is straight (“down” state) (Figure 2B), lipid moieties can insert in the lateral fenestra-

tion, thus blocking K⁺ flow (inactive conformation). Bending of M4 (“up” conformation) closes the fenestrations, preventing lipid insertion, and leading to a conducting state of the channel.²⁷ In alternative models, channel activation involves conformational transitions at the selectivity filter.²⁴ However, the possibility that multiple mechanisms may contribute to the control of K⁺ flux in response to different stimuli cannot be ruled out. To explore the structural consequences of the p.Ala172Glu and p.Ala244Pro substitutions, molecular dynamics simulations were performed (Supplemental Methods), starting from the structure of wild-type KCNK4 with one of the M4 helices (M4_B) in the up state (PDB: 4WFE)²⁷ embedded in a lipid bilayer. In agreement with the lateral fenestration-based model of gating, during the trajectory performed in the absence of channel-activating stimuli, the M4_B helix of the wild-type (WT) protein evolved toward the down conformation (the same straight structure was maintained for the M4_A helix) (Figure S2). Down conformations were populated by both helices also in the p.Ala172Glu mutant. In contrast, in the p.Ala244Pro channel, both helices attained an up conformation, in agreement with the helix-breaking properties of Pro residues.³⁴ The effect of the amino acid substitutions on the opening/closing of lateral fenestrations was also investigated. The lateral fenestrations were significantly less open in the p.Ala244Pro and p.Ala172Glu mutants compared to the WT protein (Figure 2C). By taking a reference value of 2 Å (i.e., the size of a methane molecule to represent the size of a lipid chain) as cut-off, the lateral fenestrations of WT, p.Ala172Glu, and p.Ala244Pro structures were open for 27%, 12%, and 0.2% of the time, respectively. In the model of gating based on lateral fenestrations, this finding suggests basal activation in both mutants. By contrast, no significant differences were observed in the selectivity filter region (Figure S3). Of note, in the simulation of p.Ala172Glu, the lateral fenestrations were closed for a

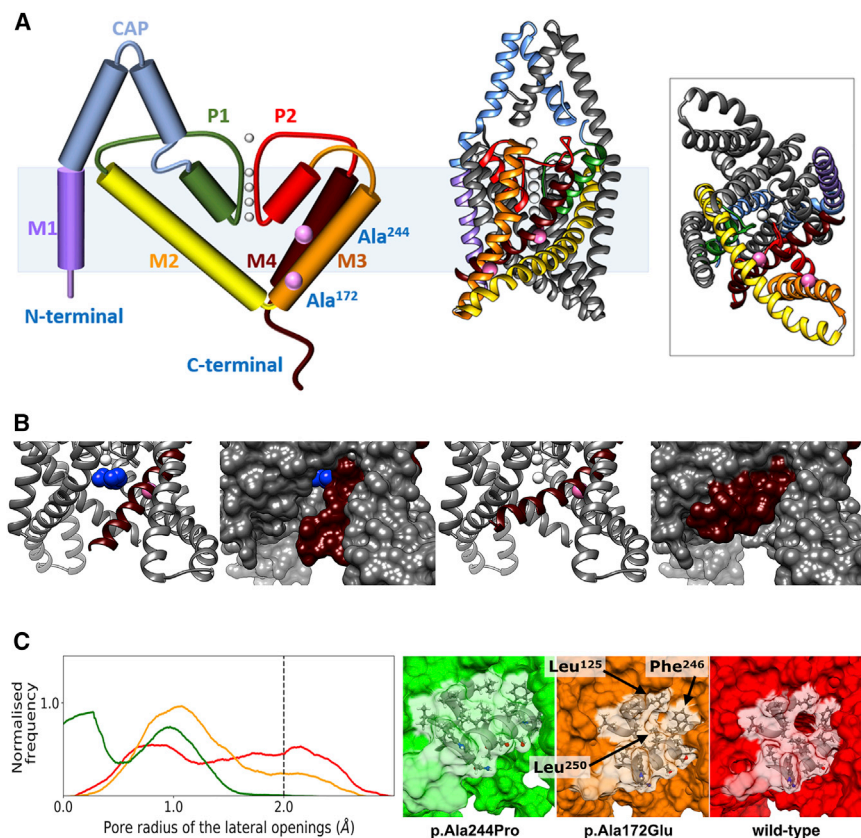


Figure 2. KCNK4 Structure and Location and Structural Consequences of Disease-Causing Mutations

(A) KCNK4 is a homodimeric channel. The schematic structure of the monomer is shown with the cytoplasmic side pointing down (left). Each subunit comprises an extracellular cap covering the pore, four transmembrane helices (M1 to M4), and two pore domains (P1 and P2) constituting the selectivity filter. K^+ ions are shown as white spheres. Locations of mutated residues are highlighted by pink spheres. The crystallographic structure of the KCNK4 dimer (PDB: 4WFF) is also shown (lateral view, middle; as seen from the cytoplasm, right). One monomer is colored with the same code of the scheme, while the other monomer is reported in gray.

(B) Structure of the KCNK4 channel in the two conformational states with open and closed lateral fenestrations (PDB: 4WFF and 4WFE, left and right panels, respectively). Only helix M4 and residue Ala²⁴⁴ are highlighted in dark red and pink, respectively. K^+ ions are shown as white spheres, while the decane molecule inserted in the lateral intramembrane fenestration and blocking the channel is shown as blue spheres. The protein is reported in both ribbon and surface representations, to illustrate the open and closed states of the fenestration that allow or avoid the entrance of the aliphatic molecule.

(C) Structural impact of the p.Ala244Pro and p.Ala172Glu amino acid substitutions, as observed in the molecular dynamics (MD) simulations. Histograms of the pore radius of the two lateral openings, observed in the MD simulations (p.Ala244Pro [green], p.Ala172Glu [orange], and WT [red]) (left). The vertical dashed line indicates the radius of a methane molecule (~ 2.0 Å). Lateral opening in the conformation that best represents those observed in the MD simulations are also shown (right). The fenestration is viewed from the lipid-exposed external surface and helices M4 and M2 are shown in transparency. Residues Leu¹²⁵, Phe²⁴⁶, and Leu²⁵⁰ involved in the hydrophobic cluster occluding the fenestration are shown in ball-and-stick representation.

significant fraction of the trajectory, even though both helices were in the down conformation (Figure 2C), suggesting that sealing of the lateral openings is more complex than simple helix bending.²⁷ This occlusion resulted from the formation of a hydrophobic cluster involving the side chains of Leu¹²⁵, Phe²⁴⁶, and Leu²⁵⁰. In the p.Ala172Glu mutant, the substitution induced the formation of an inter-domain salt bridge between Glu¹⁷² (M3 helix) and Arg¹⁴⁷ (M2 helix) (Figure S4). The strengthened salt bridge network between the M2 and M3 helices might be responsible for the closing of the fenestration, due to the multiple interactions among helices M2, M3, and M4.

To investigate experimentally the predicted activating effect of the two identified *KCNK4* mutations, their impact on protein function was assessed by patch-clamp experiments (Supplemental Methods) in transfected Chinese hamster ovary (CHO) cells. Nucleotide substitutions resulting in the p.Ala244Pro and p.Ala172Glu amino acid changes were introduced into the *KCNK4* cDNA (clone KT4.1a) cloned in a pcDNA3 vector (Invitrogen), using the QuikChange Site-Directed Mutagenesis Kit (Agilent Technologies). Cells were transfected with WT or mutant human *KCNK4* cDNA (400 ng/mL or 80 ng/mL as final concentration; co-expression assays: 80 ng/mL, each channel plasmid, resulting in a

total of 160 ng/mL channel cDNA), and cDNA encoding EGFP-N1 (Clontech), using Lipofectamine 2000 (Invitrogen). In the whole-cell mode, we recorded outward-rectifying currents in cells expressing WT *KCNK4*, which became evident at positive potentials. Membrane currents recorded from cells transfected with the mutant channels were much larger and already prominent in the negative potential range (Figures 3A and 3B). p.Ala244Pro *KCNK4* channels mostly lacked a voltage-dependent initial current increase, resembling maximally stimulated WT *KCNK4* channels.³² Voltage ramps were used to evaluate current amplitude at 0 mV and conductance at -80 mV, encompassing the most important physiological voltage range. Expression of the mutant *KCNK4* channels, as well as their co-expression with WT *KCNK4*, resulted in significantly increased current amplitudes compared to WT channels (Figures 3C, 3D, and S5), documenting the dominant impact of mutations. Current reversal was close to -80 mV and demonstrated preserved K^+ selectivity of both mutant channels. Since the whole-cell mode is regarded as the only configuration of the patch clamp-technique that exerts no tension on the cell membrane,³⁵ the observed differences reflect an impressive gain of function of the mechanically unstimulated *KCNK4* channel induced by both point mutations.

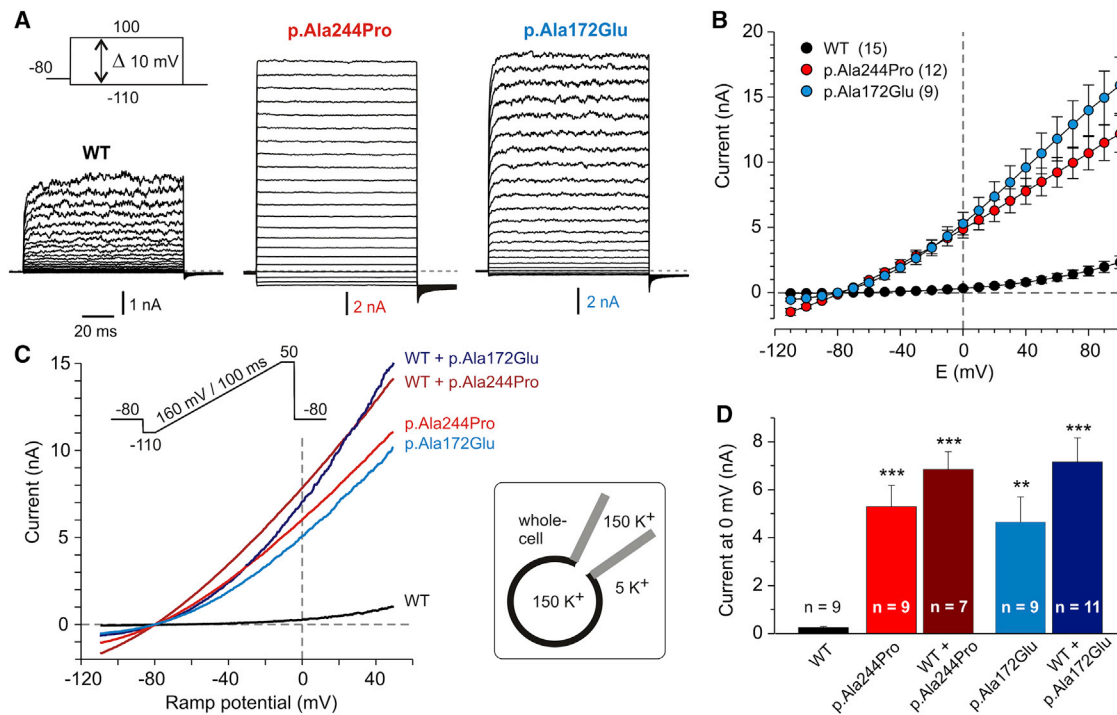


Figure 3. Whole-Cell Current Recordings from CHO Cells Expressing Wild-Type or Mutant KCNK4 Channels

(A) Representative current recordings elicited with the indicated pulse protocol consisting of 100 ms voltage steps to potentials between -110 and 100 mV in cells expressing the wild-type (WT) or mutant (p.Ala244Pro or p.Ala172Glu) KCNK4 channels. (B) The I/V-plot shows means \pm SEM of current amplitudes recorded with the voltage step protocol. Number of experiments is given in parentheses. Cell transfections were performed using a 1:10 predilution of KCNK4 cDNA (final concentration 400 ng/mL). (C) I/V-plots of representative KCNK4 current recordings elicited with the ramp protocol shown as inset. Cells were previously transfected or co-transfected with cDNA coding for WT and mutant KCNK4 cDNA using a predilution of 1:50 for each channel cDNA (final concentration 80 ng/mL and for co-transfection, a total of 160 ng/mL). (D) Means \pm SEM of the current amplitude at 0 mV ramp potential. One-way ANOVA with post hoc Bonferroni t testing yielded significant (** $p < 0.01$, *** $p < 0.001$) differences compared to WT data. A more detailed analysis of the whole-cell coexpression experiments is shown in Figure S5.

Mechanosensitivity of the different KCNK4 channels was investigated in outside-out experiments. WT KCNK4 channels were activated by positive pressure applied through the patch pipette, and the effect often increased with repetitive stimulation and with time (Figures 4A and 4B). Maximal activation resulted in an increase in current amplitudes to almost hundredfold of the initial value (Figures 4C and 4D). In most experiments, the K^+ current generated by maximally activated WT KCNK4 channels in the small membrane patch exceeded the amplitude of the corresponding whole-cell current. Outside-out patches from cells expressing each of the KCNK4 mutants exhibited higher initial current amplitude at 0 mV and higher basal K^+ conductance. Remarkably, the effect of pressure stimulation was significantly impaired in patches containing these mutants (Figures 4 and S6). Pressure-induced changes in current amplitude were absent in most experiments on p.Ala244Pro KCNK4 channels, and only a small increase in current amplitude with pressure application was documented for the p.Ala172Glu mutant. Coexpression experiments with WT and p.Ala172Glu KCNK4 channels resulted in slightly more pronounced pressure-induced channel activation,

but the effects were significantly smaller than for the WT channels (Figure S6C).

In addition to their mechanosensitivity, K2P channels of the TRAAK/TREK subfamily are sensitive to certain lipids.^{12,13} Specifically, KCNK4 is activated by arachidonic acid and polyunsaturated fatty acids. Accordingly, application of a high concentration of arachidonic acid (20 μ M) resulted in a huge increase in WT KCNK4 currents recorded in the whole-cell configuration (Figures 5A and 5D). Using the identical experimental approach, both KCNK4 mutants were found to lack the impressive channel activation in response to arachidonic acid (Figures 5B–5D), which likely reflects their maximal activation basally.

Measurements in the cell-attached configuration with undisturbed intracellular milieu and intact cytoskeleton gave qualitatively similar results (Figures S7A–S7C), further supporting the gain of function of the unstimulated mutant channels and their impaired mechanosensitivity. Of interest, the I/V relation showed pronounced inward rectification in most cell-attached measurements with the p.Ala244Pro mutant, while this feature was rarely (p.Ala172Glu) or never (WT) observed in cells expressing the other KCNK4 channels (Figures S7D and S7E). As

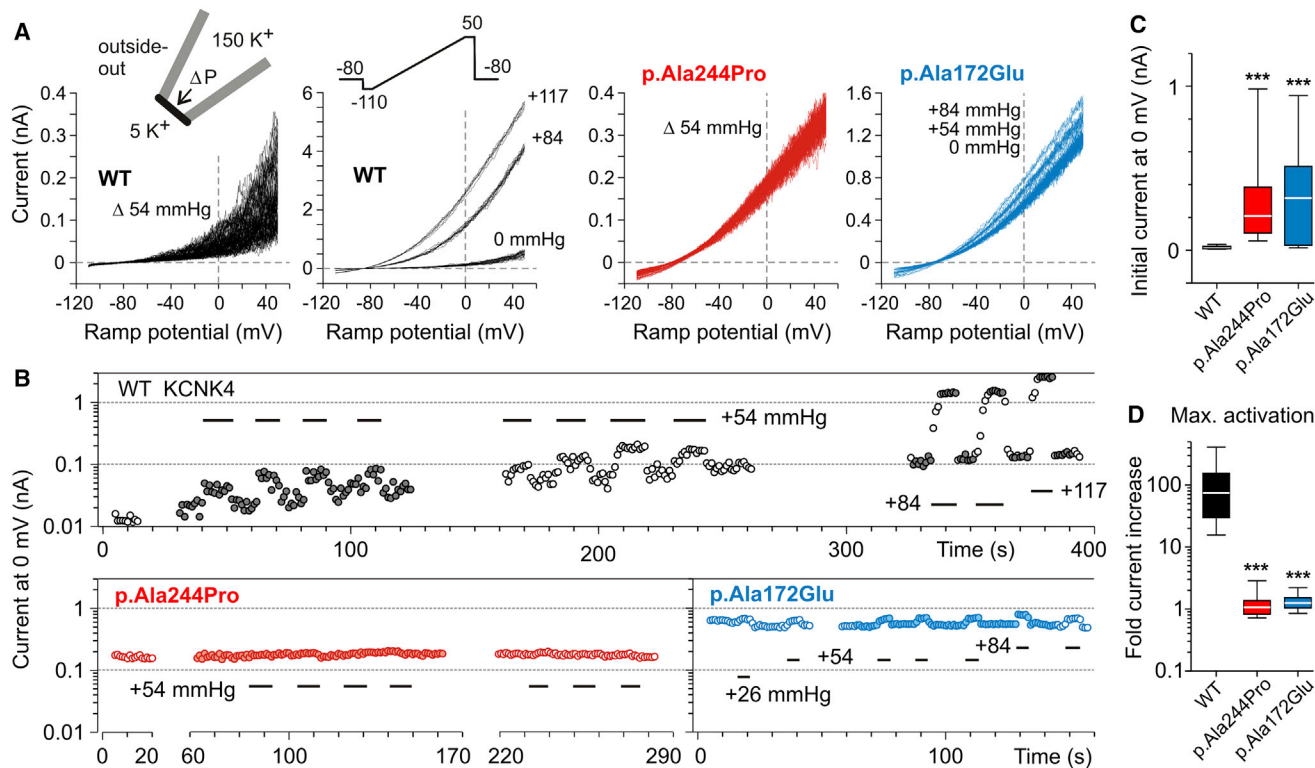


Figure 4. Current Recordings in the Outside-Out Patch-Clamp Configuration from CHO Cells Expressing Wild-Type or Mutant KCNK4 Channels

(A) Overlay of I/V plots of membrane currents repeatedly elicited by the illustrated ramp protocol with intermittent application of positive pressure. Data of a representative experiment on a cell expressing wild-type (WT) KCNK4 (both left) and data of experiments with p.Alc244Pro or p.Alc172Glu KCNK4 channels (right).

(B) Time course of current amplitudes measured at 0 mV ramp potential with intermittent mechanical stimulation; data correspond to the three experiments shown in (A). The filled symbols indicate the illustrated I/V traces. Please note the logarithmic scale used to visualize the time- and pressure-dependent changes.

(C) Analysis of current recordings directly after the establishment of the outside-out configuration. Boxplot of the current amplitudes at 0 mV ramp potential. Data from experiments with cDNA predilution 1:10 for WT KCNK4 (n = 10) and the p.Alc244Pro (n = 11) and p.Alc172Glu (n = 15) KCNK4 mutants.

(D) Analysis of maximal time- and pressure-induced changes in KCNK4 current amplitudes. Combined data from experiments using 1:10 or 1:50 cDNA predilution for transfection (WT KCNK4, n = 16; p.Alc244Pro, n = 13; p.Alc172Glu, n = 19). Fold current increase was calculated for each experiment as ratio of the maximal (with pressure) to the initial (without pressure) current amplitude at 0 mV. Please note the logarithmic scale of this parameter. Bot plot whiskers (C and D) indicate the 10/90 percentiles.

Statistical analysis (C and D): Kruskal-Wallis tests yielded significant differences between groups (ANOVA on ranks: p < 0.001); post hoc Dunn's testing yielded significant differences compared to WT data; significance levels were determined with the Wilcoxon-Mann-Whitney test (***p < 0.001). A more detailed analysis of the outside-out experiments is shown in Figure S6.

inward rectification of activated KCNK channels with inverted K⁺ concentration gradient has been reported,³² the degree of inward rectification is likely to mirror the level of intracellular K⁺ depletion. Deleterious effects of substantial K⁺ loss associated with high p.Alc244Pro KCNK4 expression levels are suggested by a lack of cells with bright EGFP fluorescence (Figure S7F). This “negative selection” most probably biased the results of the electrophysiological measurements, leading to an underestimation of the channel-activating effect promoted by the p.Alc244Pro substitution. Overall, the functional data are in agreement with the MD findings, and similarly to mechanical stimulation,^{27,28,31} both mutations are suggested to result in enhanced closing of the lateral fenestrations, favoring channel opening. This can readily explain the high basal activity, as well as the impaired mechano-

sensitivity of the mutant channels. Of note, also arachidonic acid failed to activate the disease-causing mutant channels, suggesting that both mutations promote activation of the channel basally, which cannot be further increased by stimuli involving a similar mechanism of channel activation.

While the role of K2P channels in controlling the membrane potential makes them potential players in a wide array of cellular processes, only subtle alterations in physiologic processes have been linked to dysfunction of these channels.³⁶ Our findings provide evidence that gain-of-function mutations in *KCNK4* cause a distinctive neurodevelopmental syndrome, for which we propose the acronym FHEIG (facial dysmorphism, hypertrichosis, epilepsy, intellectual disability/developmental delay, and gingival overgrowth). While additional case subjects are

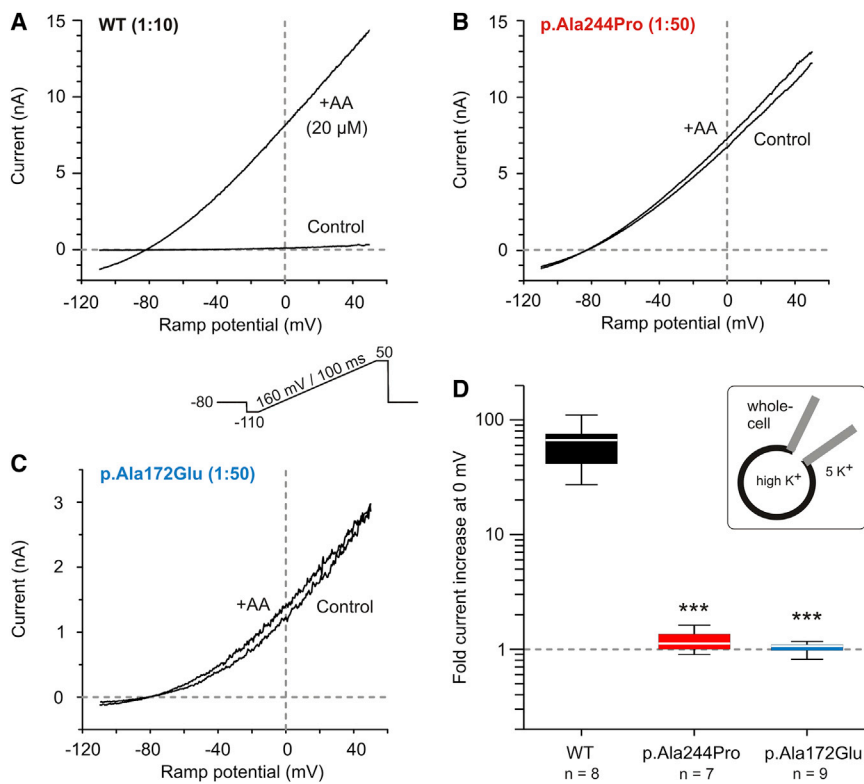


Figure 5. The Basally Activated p.Ala244Pro and p.Ala172Glu KCNK4 Mutants Do Not Further Respond to Arachidonic Acid (AA) Stimulation

(A–C) I/V-plots of current traces recorded in the whole-cell configuration with a ramp protocol (beneath A) from cells previously transfected with cDNA coding for wild-type (WT) KCNK4 (A; cDNA predilution 1:10), and p.Ala244Pro (B) or p.Ala172Glu (C) KCNK4 (each mutant: cDNA predilution 1:50). Control current traces (just before application of AA) and traces illustrating maximal current amplitudes after application of 20 μM AA are superimposed. (D) Analysis of AA-induced changes. Results are presented as box plot (whiskers indicate the 10/90 percentiles). Please note the logarithmic scale. Application of 20 μM AA resulted in a slowly developing, impressive activation of WT KCNK4 channels (maximal current amplitude at 0 mV in the time period 2–20 min after AA application relative to the value just before AA application is given as fold current increase; median = 66.7). Both mutant channels showed a significantly impaired response to AA (p.Ala244Pro, fold current increase: median = 1.12; p.Ala172Glu, fold current increase: median = 1.06). Asterisks denote significant differences compared to WT data (ANOVA on ranks and post hoc Dunn's testing; ***p < 0.001).

required to delineate more accurately the clinical variability associated with activating *KCNK4* mutations, the specific association of features and distinctive facies support the view that this condition represents a novel nosologic entity. Based on the three identified affected subjects, the major features characterizing this disorder are reminiscent of the phenotypic continuum associated with activating mutations in the voltage-gated K⁺ channel *KCNH1* (MIM: 603305)^{8,9} and disorders caused by mutations in *ABCC9* (MIM: 601439) and *KCNJ8* (MIM: 600935), two genes encoding ATP-sensitive potassium channel subunits with defective function in Cantù syndrome.^{10,11} In subjects with *KCNK4* mutations, the clinical phenotype is characterized by a significant evolution of the craniofacial features with age, and the condition should be considered in differential diagnosis with other disorders (Table S3). Neonatally, it resembles Wiedemann-Steiner syndrome (MIM: 605130) to some extent, while later the phenotype becomes more similar to Temple-Baraitser syndrome (MIM: 611816) and mild forms of Cantù (MIM: 239850) and Coffin-Siris (MIM: 135900) syndromes. Similarly to what is observed in these syndromes, the three affected subjects with *de novo* *KCNK4* mutations show variable developmental delay and cognitive impairment, ranging from a mild speech delay and disorganized pattern of development (individual 2) to an extremely severe ID (individual 1). In contrast to other K2P channels, *KCNK4* appears to be almost exclusively expressed in neuronal cells of the central and peripheral

nervous system and in the retina (see GTEx database); so, the finding of its pleiotropic impact is unexpected. In rodent peripheral somatosensory neurons, *KCNK4* appears to modulate thermo- and mechano-sensation and the respective threshold to nociception.³⁷ Laser-evoked potentials assessed in subjects 1 and 2 did not provide any aberrant pattern, suggesting no gross dysregulation of temperature and pressure sensitivity.

Depending upon the gating behavior of a given K⁺ channel and its cellular and subcellular expression profile in the brain, intellectual impairment and seizures can result from either loss-of-function or gain-of-function mutations.^{2,5,7–11,38} Notably, gingival overgrowth is a major feature in subjects with gain-of-function mutations in *KCNH1*,^{8,9} *KCNQ1*,³⁹ and *KCNK4* (present study), which consistently result in significantly elevated K⁺ conductance at more negative potentials. Of note, *Kcnk4*^{-/-} mice exhibit neither obvious developmental abnormalities nor increased susceptibility to seizures or deficits in cognition, touch, vision, and hearing.⁴⁰ Thus, loss of *KCNK4* function is likely compensated for by other members of the K2P family or its relevance is limited to pathophysiological conditions like brain ischemia.^{41,42} Accordingly, the two disease-causing *KCNK4* mutations resulted in an impressive gain of function, indicated by a dramatically increased basal K⁺ conductance. Of note, the sustained high K⁺ conductance responsible for the clinical features and symptoms observed in FHEIG syndrome is expected to drain K⁺ out of cells that exhibit considerable depolarizing currents.

This can result in intracellular K⁺ depletion and increased interstitial K⁺ concentration, with a depolarizing effect also on neighboring cells.

Taken together, our findings characterize a channelopathy that is caused by hyperactivation of KCNK4 channels. While the molecular mechanisms controlling K_{2P} channel function are still subjects of debate, the present *in silico* and *in vitro* data consistently support the relevance of the closing of lateral fenestrations to channel gating,^{24,43} and suggest that helix bending is not the only conformational transition controlling the state of lateral fenestrations in K_{2P} channels.

Accession Numbers

The accession numbers for the mutations reported in this paper are ClinVar: SCV000804240 (GenBank: NM_001317090.1; c.515C>A) and SCV000804241 (GenBank: NM_001317090.1; c.730G>C).

Supplemental Data

Supplemental Data include Supplemental Methods, Case Reports, seven figures, and three tables and can be found with this article online at <https://doi.org/10.1016/j.ajhg.2018.09.001>.

Acknowledgments

The authors wish to thank the participating families; Thomas Baukowitz (Institute of Physiology, Kiel University, Kiel) for providing the KCNK4 cDNA; Fanny Kortüm, Frederike L. Harms, and Inka Jantke (Institute of Human Genetics, University Medical Center Hamburg-Eppendorf, Hamburg) for generating KCNK4 expression constructs; and Serenella Venanzi (Istituto Superiore di Sanità, Rome) and Annett Hasse (Institute of Cellular and Integrative Physiology, University Medical Center Hamburg-Eppendorf, Hamburg) for technical support. This work was supported, in part, by Fondazione Bambino Gesù (Vite Coraggiose to B.D. and M.T.) and the Italian Ministry of Health (Ricerca Corrente 2017 and 2018 to M.L.D., M.C.D., A.C., and M.T.). G.B. acknowledges PRACE (Partnership for Advanced Computing in Europe, grant 2017174118), and M.T. and G.B. acknowledge CINECA for the computational resources.

Declaration of interests

The authors declare no competing interests.

Received: July 6, 2018

Accepted: August 31, 2018

Published: October 4, 2018

WEB Resources

CADD, <https://cadd.gs.washington.edu/>
ClinVar, <https://www.ncbi.nlm.nih.gov/clinvar/>
GenBank, <https://www.ncbi.nlm.nih.gov/genbank/>
gnomAD Browser, <http://gnomad.broadinstitute.org/>
GTEX Portal, <https://gtexportal.org/home/>
InterVar, <http://wintervar.wglab.org/>
M-CAP, <http://bejerano.stanford.edu/mcap/>

OMIM, <http://www.omim.org/>

RCSB Protein Data Bank, <http://www.rcsb.org/pdb/home/home.do>

References

1. Hille, B. (2001). Ion channels of excitable membranes (Sinauer Associates).
2. Tian, C., Zhu, R., Zhu, L., Qiu, T., Cao, Z., and Kang, T. (2014). Potassium channels: structures, diseases, and modulators. *Chem. Biol. Drug Des.* 83, 1–26.
3. Urrego, D., Tomczak, A.P., Zahed, F., Stühmer, W., and Pardo, L.A. (2014). Potassium channels in cell cycle and cell proliferation. *Philos. Trans. R. Soc. Lond. B Biol. Sci.* 369, 20130094.
4. Shieh, C.C., Coghlan, M., Sullivan, J.P., and Gopalakrishnan, M. (2000). Potassium channels: molecular defects, diseases, and therapeutic opportunities. *Pharmacol. Rev.* 52, 557–594.
5. Jentsch, T.J. (2000). Neuronal KCNQ potassium channels: physiology and role in disease. *Nat. Rev. Neurosci.* 1, 21–30.
6. Chiamvimonvat, N., Chen-Izu, Y., Clancy, C.E., Deschenes, I., Dobrev, D., Heijman, J., Izu, L., Qu, Z., Ripplinger, C.M., Vandenberg, J.I., et al. (2017). Potassium currents in the heart: functional roles in repolarization, arrhythmia and therapeutics. *J. Physiol.* 595, 2229–2252.
7. Bockenbauer, D., Feather, S., Stanescu, H.C., Bandulik, S., Zdebik, A.A., Reichold, M., Tobin, J., Lieberer, E., Sterner, C., Landouere, G., et al. (2009). Epilepsy, ataxia, sensorineural deafness, tubulopathy, and KCNJ10 mutations. *N. Engl. J. Med.* 360, 1960–1970.
8. Simons, C., Rash, L.D., Crawford, J., Ma, L., Cristofori-Armstrong, B., Miller, D., Ru, K., Baillie, G.J., Alanay, Y., Jacquinet, A., et al. (2015). Mutations in the voltage-gated potassium channel gene KCNH1 cause Temple-Baraitser syndrome and epilepsy. *Nat. Genet.* 47, 73–77.
9. Kortüm, F., Caputo, V., Bauer, C.K., Stella, L., Ciolfi, A., Alawi, M., Bocchinfuso, G., Flex, E., Paolacci, S., Dentici, M.L., et al. (2015). Mutations in KCNH1 and ATP6V1B2 cause Zimmermann-Laband syndrome. *Nat. Genet.* 47, 661–667.
10. Harakalova, M., van Harsse, J.J., Terhal, P.A., van Lieshout, S., Duran, K., Renkens, I., Amor, D.J., Wilson, L.C., Kirk, E.P., Turner, C.L., et al. (2012). Dominant missense mutations in ABCC9 cause Cantú syndrome. *Nat. Genet.* 44, 793–796.
11. Cooper, P.E., Reutter, H., Woelfle, J., Engels, H., Grange, D.K., van Haften, G., van Bon, B.W., Hoischen, A., and Nichols, C.G. (2014). Cantú syndrome resulting from activating mutation in the KCNJ8 gene. *Hum. Mutat.* 35, 809–813.
12. Fink, M., Lesage, F., Duprat, F., Heurteaux, C., Reyes, R., Fosset, M., and Lazdunski, M. (1998). A neuronal two P domain K⁺ channel stimulated by arachidonic acid and polyunsaturated fatty acids. *EMBO J.* 17, 3297–3308.
13. Feliciangeli, S., Chatelain, F.C., Bichet, D., and Lesage, F. (2015). The family of K_{2P} channels: salient structural and functional properties. *J. Physiol.* 593, 2587–2603.
14. Sepúlveda, F.V., Pablo Cid, L., Teulon, J., and Niemeyer, M.I. (2015). Molecular aspects of structure, gating, and physiology of pH-sensitive background K_{2P} and K_{ir} K⁺-transport channels. *Physiol. Rev.* 95, 179–217.
15. Niceta, M., Stellacci, E., Gripp, K.W., Zampino, G., Kousi, M., Anselmi, M., Traversa, A., Ciolfi, A., Stabley, D., Bruselles, A., et al. (2015). Mutations impairing GSK3-mediated MAF phosphorylation cause cataract, deafness, intellectual disability,

- seizures, and a Down syndrome-like facies. *Am. J. Hum. Genet.* **96**, 816–825.
16. Flex, E., Niceta, M., Cecchetti, S., Thiffault, I., Au, M.G., Capuano, A., Piermarini, E., Ivanova, A.A., Francis, J.W., Chillemi, G., et al. (2016). Biallelic mutations in TBCD, encoding the tubulin folding cofactor D, perturb microtubule dynamics and cause early-onset encephalopathy. *Am. J. Hum. Genet.* **99**, 962–973.
 17. Sferra, A., Baillat, G., Rizza, T., Barresi, S., Flex, E., Tasca, G., D'Amico, A., Bellacchio, E., Ciolfi, A., Caputo, V., et al. (2016). TBCE mutations cause early-onset progressive encephalopathy with distal spinal muscular atrophy. *Am. J. Hum. Genet.* **99**, 974–983.
 18. Kircher, M., Witten, D.M., Jain, P., O'Roak, B.J., Cooper, G.M., and Shendure, J. (2014). A general framework for estimating the relative pathogenicity of human genetic variants. *Nat. Genet.* **46**, 310–315.
 19. Jagadeesh, K.A., Wenger, A.M., Berger, M.J., Guturu, H., Stenson, P.D., Cooper, D.N., Bernstein, J.A., and Bejerano, G. (2016). M-CAP eliminates a majority of variants of uncertain significance in clinical exomes at high sensitivity. *Nat. Genet.* **48**, 1581–1586.
 20. Li, Q., and Wang, K. (2017). InterVar: clinical interpretation of genetic variants by the 2015 ACMG-AMP guidelines. *Am. J. Hum. Genet.* **100**, 267–280.
 21. Richards, S., Aziz, N., Bale, S., Bick, D., Das, S., Gastier-Foster, J., Grody, W.W., Hegde, M., Lyon, E., Spector, E., et al.; ACMG Laboratory Quality Assurance Committee (2015). Standards and guidelines for the interpretation of sequence variants: a joint consensus recommendation of the American College of Medical Genetics and Genomics and the Association for Molecular Pathology. *Genet. Med.* **17**, 405–424.
 22. Sobreira, N., Schiettecatte, F., Valle, D., and Hamosh, A. (2015). GeneMatcher: a matching tool for connecting investigators with an interest in the same gene. *Hum. Mutat.* **36**, 928–930.
 23. Tanaka, A.J., Cho, M.T., Millan, F., Juusola, J., Retterer, K., Joshi, C., Niyazov, D., Garnica, A., Gratz, E., Deardorff, M., et al. (2015). Mutations in SPATA5 are associated with microcephaly, intellectual disability, seizures, and hearing loss. *Am. J. Hum. Genet.* **97**, 457–464.
 24. Renigunta, V., Schlichthörl, G., and Daut, J. (2015). Much more than a leak: structure and function of K_{2p}-channels. *Pflugers Arch.* **467**, 867–894.
 25. Brohawn, S.G., del Marmol, J., and MacKinnon, R. (2012). Crystal structure of the human K_{2P} TRAAK, a lipid- and mechano-sensitive K⁺ ion channel. *Science* **335**, 436–441.
 26. Brohawn, S.G., Campbell, E.B., and MacKinnon, R. (2013). Domain-swapped chain connectivity and gated membrane access in a Fab-mediated crystal of the human TRAAK K⁺ channel. *Proc. Natl. Acad. Sci. USA* **110**, 2129–2134.
 27. Brohawn, S.G., Campbell, E.B., and MacKinnon, R. (2014). Physical mechanism for gating and mechanosensitivity of the human TRAAK K⁺ channel. *Nature* **516**, 126–130.
 28. Brohawn, S.G. (2015). How ion channels sense mechanical force: insights from mechanosensitive K_{2P} channels TRAAK, TREK1, and TREK2. *Ann. N Y Acad. Sci.* **1352**, 20–32.
 29. Lolicato, M., Riegelhaupt, P.M., Arrigoni, C., Clark, K.A., and Minor, D.L., Jr. (2014). Transmembrane helix straightening and buckling underlies activation of mechanosensitive and thermosensitive K(2P) channels. *Neuron* **84**, 1198–1212.
 30. Niemeyer, M.I., Cid, L.P., González, W., and Sepúlveda, F.V. (2016). Gating, regulation, and structure in K_{2P} K⁺ channels: In varietate concordia? *Mol. Pharmacol.* **90**, 309–317.
 31. Aryal, P., Jarerattanachai, V., Clausen, M.V., Schewe, M., McClenaghan, C., Argent, L., Conrad, L.J., Dong, Y.Y., Pike, A.C.W., Carpenter, E.P., et al. (2017). Bilayer-mediated structural transitions control mechanosensitivity of the TREK-2 K_{2P} channel. *Structure* **25**, 708–718.e2.
 32. Schewe, M., Nematian-Ardestani, E., Sun, H., Musinszki, M., Cordeiro, S., Bucci, G., de Groot, B.L., Tucker, S.J., Rapedius, M., and Baukrowitz, T. (2016). A non-canonical voltage-sensing mechanism controls gating in K_{2P} K(+) channels. *Cell* **164**, 937–949.
 33. Masetti, M., Berti, C., Ocello, R., Di Martino, G.P., Recanatini, M., Fiegna, C., and Cavalli, A. (2016). Multiscale simulations of a two-pore potassium channel. *J. Chem. Theory Comput.* **12**, 5681–5687.
 34. Bobone, S., Bocchinfuso, G., Park, Y., Palleschi, A., Hahm, K.S., and Stella, L. (2013). The importance of being kinked: role of Pro residues in the selectivity of the helical antimicrobial peptide P5. *J. Pept. Sci.* **19**, 758–769.
 35. Schmidt, D., del Marmol, J., and MacKinnon, R. (2012). Mechanistic basis for low threshold mechanosensitivity in voltage-dependent K⁺ channels. *Proc. Natl. Acad. Sci. USA* **109**, 10352–10357.
 36. Sabbadini, M., and Yost, C.S. (2009). Molecular biology of background K channels: insights from K(2P) knockout mice. *J. Mol. Biol.* **385**, 1331–1344.
 37. Noël, J., Zimmermann, K., Busserolles, J., Deval, E., Alloui, A., Diochot, S., Guy, N., Borsotto, M., Reeh, P., Eschalier, A., and Lazdunski, M. (2009). The mechano-activated K⁺ channels TRAAK and TREK-1 control both warm and cold perception. *EMBO J.* **28**, 1308–1318.
 38. Lehman, A., Thouta, S., Mancini, G.M.S., Naidu, S., van Slegtenhorst, M., McWalter, K., Person, R., Mwenifumbo, J., Salvarinova, R., Guella, I., et al.; CAUSES Study; and EPGEN Study (2017). Loss-of-function and gain-of-function mutations in KCNQ5 cause intellectual disability or epileptic encephalopathy. *Am. J. Hum. Genet.* **101**, 65–74.
 39. Tommiska, J., Käsäkoski, J., Skibsbjörns, L., Vaaralahti, K., Liu, X., Lodge, E.J., Tang, C., Yuan, L., Fagerholm, R., Kanters, J.K., et al. (2017). Two missense mutations in KCNQ1 cause pituitary hormone deficiency and maternally inherited gingival fibromatosis. *Nat. Commun.* **8**, 1289.
 40. Heurteaux, C., Guy, N., Laigle, C., Blondeau, N., Duprat, F., Mazzuca, M., Lang-Lazdunski, L., Widmann, C., Zanzouri, M., Romey, G., and Lazdunski, M. (2004). TREK-1, a K⁺ channel involved in neuroprotection and general anesthesia. *EMBO J.* **23**, 2684–2695.
 41. Laigle, C., Confort-Gouny, S., Le Fur, Y., Cozzone, P.J., and Viola, A. (2012). Deletion of TRAAK potassium channel affects brain metabolism and protects against ischemia. *PLoS ONE* **7**, e53266.
 42. Mirkovic, K., Palmersheim, J., Lesage, F., and Wickman, K. (2012). Behavioral characterization of mice lacking Trek channels. *Front. Behav. Neurosci.* **6**, 60. <https://doi.org/10.3389/fnbeh.2012.00060>.
 43. McClenaghan, C., Schewe, M., Aryal, P., Carpenter, E.P., Baukrowitz, T., and Tucker, S.J. (2016). Polymodal activation of the TREK-2 K_{2P} channel produces structurally distinct open states. *J. Gen. Physiol.* **147**, 497–505.